

PLANT SCIENCE

YABBY and diverged KNOX1 genes shape nodes and internodes in the stem

Katsutoshi Tsuda^{1,2*}, Akiteru Maeno¹, Ayako Otake¹, Kae Kato¹, Wakana Tanaka³, Ken-Ichiro Hibara⁴, Ken-Ichi Nonomura^{1,2}

Plant stems comprise nodes and internodes that specialize in solute exchange and elongation. However, their boundaries are not well defined, and how these basic units arise remains elusive. In rice with clear nodes and internodes, we found that one subclade of class I *knotted1-like homeobox* (*KNOX1*) genes for shoot meristem indeterminacy restricts node differentiation and allows internode formation by repressing *YABBY* genes for leaf development and genes from another node-specific *KNOX1* subclade. *YABBY*s promote nodal vascular differentiation and limit stem elongation. *YABBY* and node-specific *KNOX1* genes specify the pulvinus, which further elaborates the nodal structure for gravitropism. Notably, this *KNOX1* subclade organization is specific to seed plants. We propose that nodes and internodes are distinct domains specified by *YABBY*-*KNOX1* cross-regulation that diverged in early seed plants.

Stems are plant shoot axes that consist of nodes and internodes, which define stem architecture. Nodes are the attachment points between leaves and stems, where intricate vascular networks allow water and solute exchange (1). Internodes develop between nodes and undergo rapid elongation to lift leaves and inflorescences for light capture and pollen or seed dispersal. Regulation of stem elongation is important for crop improvement, as exemplified by the semidwarf mutations used in the Green Revolution of the 1960s (2). Despite its importance, stem development has been poorly studied compared with other major organs owing to the lack of clear external landmarks in many species (3). Therefore, the nature of the developmental programs required to specify each domain of the stem remains poorly understood.

Grasses are excellent models for studying stem development because the distinctions among nodes, internodes, and neighboring organs are clear (Fig. 1A, fig. S1, and supplementary text) (4, 5). The stem is produced from the shoot apical meristem (SAM) as a part of the phytomer, which is a developmental unit comprising a leaf, stem, and axillary bud. In rice, we recently reported that the determination of cell fate for each organ or domain in a phytomer occurs in a stepwise fashion, with nodes being established earlier than internodes (5). In addition, internodal cells that express mitotic markers originate several nodes away from the apex of *Arabidopsis* in-

florescences (6). Hence, nodes begin to develop earlier than internodes. However, the underlying molecular mechanisms remain elusive.

Knotted1-like homeobox (*KNOX1*) and *BELL1-like homeobox* (*BLH*) transcription factors (TFs) play important roles in shoot axes in land plants (7). In angiosperms, *KNOX1* and *BLH* genes are essential for SAM maintenance and stem elongation (7–12). Studies in *Arabidopsis* have reported that these genes promote stem elongation by repressing multiple regulators of lateral organs and organ boundaries (13–17). However, the developmental context of the stem behind these interactions remains unclear.

Leaves in seed plants evolved from leafless, three-dimensionally branching sporophyte axes gradually; the determinacy of lateral branching axes preceded the establishment of adaxial-abaxial polarity and extensive lamina growth (18, 19). *YABBY* family TFs, which became prevalent only in seed plants, are involved in all these aspects of leaf development (20–23). Therefore, the integration of *YABBY* TFs into the shoot axis program was a key event in leaf acquisition in seed plants (21, 24). Given the nature of nodes as leaf attachment points, developmental programs for stems and leaves may converge at nodes. We report here that distinct members of the *KNOX1* family that diverged in early seed plants play central roles in node–internode patterning, partly by antagonizing and cooperating with *YABBY* genes.

Results

KNOX1 and *BLH* genes restrict node differentiation

We performed genetic analyses of rice *KNOX1* genes, *Oryza sativa* *homeobox15* (*OSH15*) and *OSH1*, which belong to the *BREVIPEDICELLUS* (*BP*) subclade (Fig. 1B). The expression of another gene, *OSH43*, was exceptionally low (fig. S2A). Therefore, we focused on the first two genes. Loss-of-function mutants of *OSH15* (known as *d6* mutants) show dwarfism with shortened inter-

nodes, similar to the *Arabidopsis* *bp* mutants (Fig. 1, C and D, and fig. S2) (8, 10). *OSH1* is essential for SAM maintenance; however, its role in stem development remains unknown (25). Therefore, we generated *d6 osh1/+* double mutants (*d6 osh1* double homozygotes are embryonic lethal) (25). They showed a pronounced short-stem phenotype, indicating that *OSH1* is also important for stem development (Fig. 1, C and D, and fig. S2). Next, we observed mutants of the *BLH* cofactor genes *VERTICILLATE RACHIS* (*VR*) and *RI-Like* (*RIL*), which are closely related to *Arabidopsis* *PENNYWISE* (*PI*, 26). Their single and double mutants showed a range of dwarfism, and *ri/+ ril* mutants developed very short stems like *d6 osh1/+* (*ri ril* double homozygotes are also embryonic lethal) (Fig. 1, C and D, and fig. S2) (26).

To examine the cause of these defects, we observed young stems using micro-computed tomography (micro-CT), which visualizes external and internal three-dimensional (3D) structures (12). Externally, *d6* mutants depicted enlarged nodes and shortened internodes compared with the wild type, and *d6 osh1/+* and *ri/+ ril* lacked clear internodes (Fig. 1E). *ri/+ ril* mutants often lacked axillary buds, similar to maize *blh12 blh14* double mutants (Fig. 1E) (12). Internally, enlarged vascular bundles (EVBs), the node-specific vasculatures specializing in solute exchange (fig. S1 and supplementary text), expanded compared with those in the wild type, and ectopic EVBs were formed in the foot in *d6* mutants (Fig. 1, E to G). The latter phenotype is particularly important because if the dwarfism is caused simply by the reduced meristematic activity, the foot should remain unchanged. Therefore, the developmental program(s) for EVBs were likely activated ectopically in the *d6* foot. Notably, in *d6 osh1/+* and *ri/+ ril* double mutants, EVBs occupied the entire stem length (Fig. 1, F and G). Moreover, features in the wild-type nodes, including a less-lignified epidermis, a highly lignified endodermis, and diffusing vascular bundles (fig. S1), were observed along stems of these double mutants (Fig. 1G). Thus, *KNOX1* and *BLH* TFs restrict node differentiation and allow internode formation.

Ectopic YABBY expression caused dwarfisms in knox1 and blh mutants

To elucidate the molecular functions of *OSH15*, we compared transcriptomes of wild-type and *d6* stems (fig. S3). By clustering differentially expressed genes among tissues and genotypes ($k = 7$), we identified two large clusters with distinct trends (fig. S3B). In one cluster (cluster 3), genes were abundantly expressed in intercalary meristems (IMs) (supplementary text) in the wild type and down-regulated in *d6*. This cluster included many genes involved in the cell cycle and DNA synthesis, as well as genes whose mutations are known to cause dwarfism (fig. S3, C to E) (27–30), suggesting that genetic

¹Plant Cytogenetics Laboratory, Department of Gene Function and Phenomics, National Institute of Genetics, Mishima, Shizuoka 411-8540, Japan. ²Department of Genetics, School of Life Science, Graduate University for Advanced Studies, Mishima, Shizuoka 411-8540, Japan.

³Graduate School of Integrated Sciences for Life, Hiroshima University, Higashi-Hiroshima, Hiroshima 739-8528, Japan.

⁴Graduate School of Agricultural Regional Vitalization, Kibi International University, Minamiawaji, Hyogo 656-0484, Japan.

*Corresponding author. Email: katsuda@nig.ac.jp

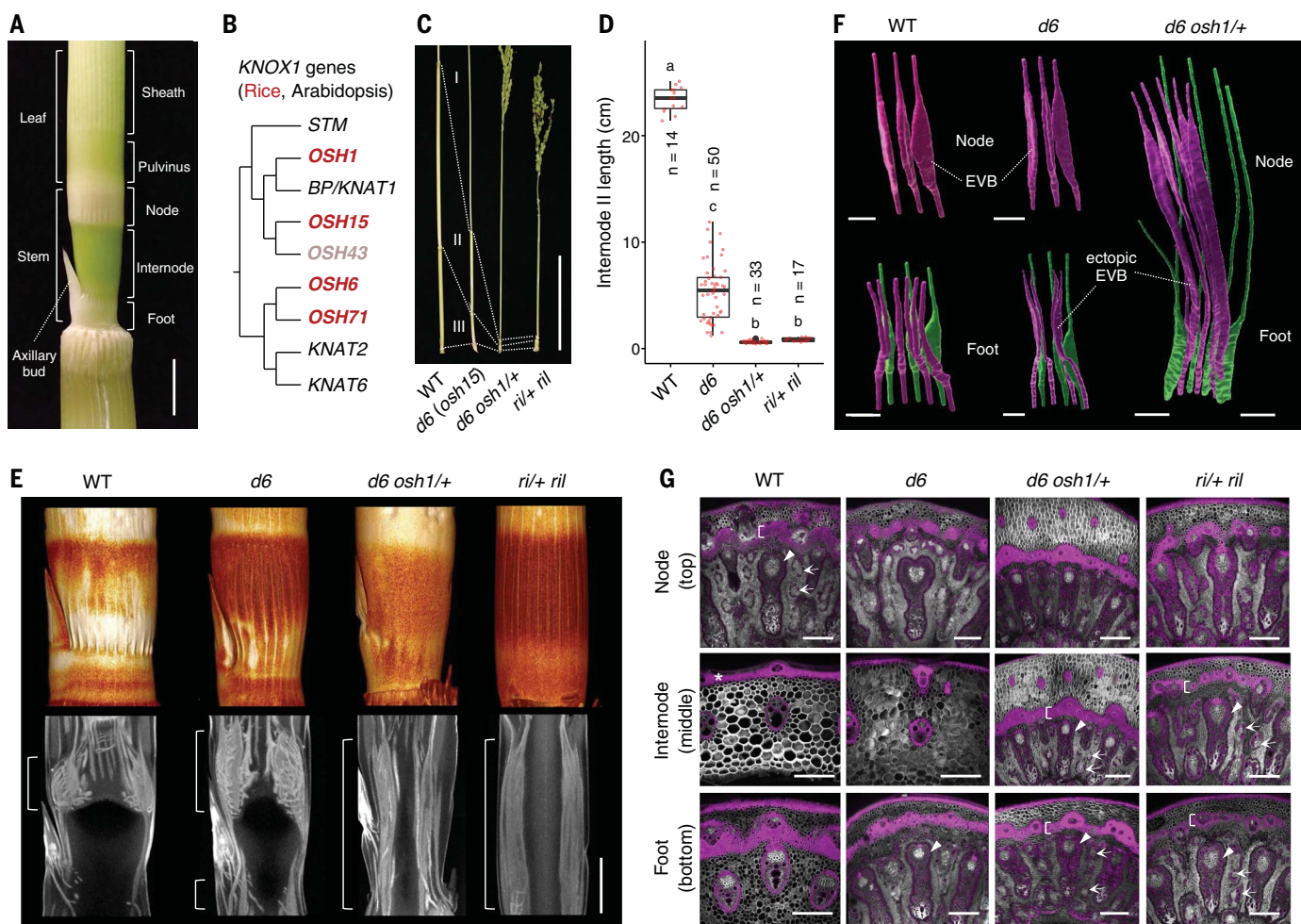


Fig. 1. *knox1* and *blh* mutants showed enlarged nodes and diminished internodes. (A) Young rice stem. **(B)** Cladogram of rice (red) and *Arabidopsis* (black) *KNOX1* genes. **(C)** Mature stem phenotypes. Internodes are numbered from the top. WT, wild type. **(D)** Internode II length at maturity. Different letters indicate significant differences ($P < 0.05$, Tukey-Kramer test). Red dots, each sample; black dots, outliers; center line, median; box limits, upper and lower quartiles; whiskers, 1.5× interquartile range. **(E)** Micro-CT images of young stems. The upper and lower panels represent external (3D volume rendering in which

regions with higher x-ray absorption were shown in brighter color) and internal views, respectively. Brackets are regions with EVBs. **(F)** Vein structures extracted from micro-CT data. Veins in magenta are of the flag leaf phytomer, and those in green belong to one phytomer below. **(G)** Transverse sections of mature stems stained with basic fuchsin (magenta) and calcofluor white (gray). Arrows, arrowheads, and brackets indicate diffusing vascular bundles, EVBs, and lignified endodermal layers, respectively. An asterisk indicates a highly lignified epidermal layer in WT internodes. Bars, 5 mm (A), 10 cm (C), 2 mm (E), 1 mm (F), and 200 μ m (G).

pathways for internode growth were globally repressed in *d6* mutants. In another cluster (cluster 2), genes were up-regulated and their expression domains expanded from the node and foot toward IMs in *d6* mutants (fig. S3B). This cluster encompassed many genes associated with the cell wall and lignin pathways (fig. S3, C and D). These trends were consistent with the enlarged nodes and diminished internodes of *d6* mutants and with known *KNOX1* functions to repress lignin synthesis (31).

To identify the regulatory factors involved in dwarfism, we explored TFs whose expression was altered in *d6*. The *YABBY* family was notable because most members were up-regulated in *d6* mutants (Fig. 2A and fig S3, C, F, and G). *YABBY* TFs are well-characterized regulators of

leaf development (20–23). Notably, antagonistic genetic interactions between the *YABBY* gene *FILAMENTOUS FLOWER* (*FIL*) and *KNOX1* genes in the SAM and stems were previously reported in *Arabidopsis* (14, 20). Therefore, we knocked out five rice *YABBY* genes. Mutations in two closely related *FIL*-like genes, *TONGARI-BOUSHI1* (*TOBI1*) and *TOB2* (fig. S3H) (32, 33) greatly recovered internode growth in the *d6* background (Fig. 2, B and C), whereas mutations in other genes had minor effects (fig. S4A). In addition, ectopic EVBs in *d6* foot were suppressed by *tob2* mutations (fig. S4B). Therefore, we focused on *TOB1* and *TOB2* in subsequent analyses. *tob1 tob2* double mutants were shorter than the wild type but still developed normal nodes and internodes (fig. S5 and S6).

Notably, *tob1 tob2* mutations suppressed the extreme dwarfism in both *d6 osh1/+* and *ri/+ ril* backgrounds (Fig. 2, B and C, and figs. S4 to S6). Histological observations confirmed that internode formation was restored in *d6 osh1/+ tob1 tob2* quadruple mutants (Fig. 2D). Conversely, overexpressors of *TOB1* or *TOB2* formed very short stems with ectopic EVBs (fig. S4, E to Q). Hence, the misregulation of *TOB1* and *TOB2* causes severe dwarfism in *knox1* and *blh* mutants.

KNOX1 and *BLH* repress *TOB1/2* in internode vasculatures

tob1 tob2 double mutants showed spikelet defects, as reported previously (32), and the introduction of the genomic *TOB1-GFP* (green fluorescent protein) or *TOB2-GFP* constructs recovered

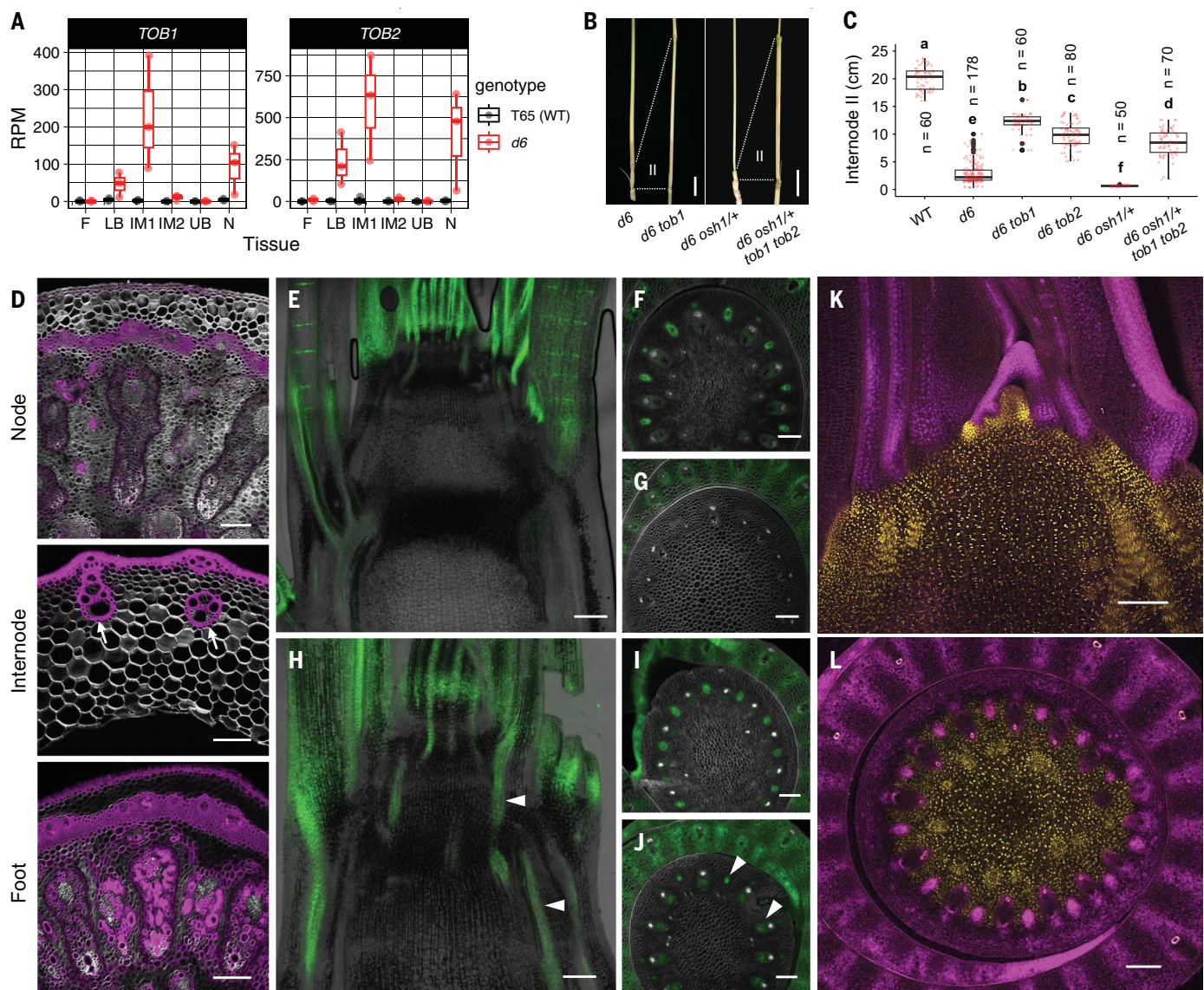


Fig. 2. Ectopic expression of TOB1 and TOB2 caused dwarfisms in knox1 mutants. (A) Expression levels of *TOB1* and *TOB2* in the transcriptome data. F, foot; IM1, intercalary meristem1; IM2, intercalary meristem2; LB, lower boundary; N, node; UB, upper boundary. Samples were defined in fig. S3A. (B) Mature internode II of *knox1* and *yabby* mutants. (C) Internode II length at maturity. Different letters indicate significant differences ($P < 0.05$, Tukey–Kramer test). (D) Transverse sections of mature stems in *d6 osh1^{+/} tob1 tob2* quadruple mutants stained with basic fuchsin (magenta) and calcofluor white (gray). Arrows indicate normal internode veins restored in the quadruple mutant. (E to

J) GFP fluorescence of *gTOB1-GFP* in the WT (E to G) and *d6* mutants (H to J). (E) and (H) show longitudinal sections of shoot apices; (F) and (I) show transverse sections of young nodes; (G) and (J) show transverse sections of young internodes. Arrowheads indicate ectopic expression in internodes. GFP channel (green) was merged with bright field [(E) and (H)] or calcofluor white [gray in (F), (G), (I), and (J)]. (K and L) Longitudinal (K) and transverse (L) sections of *gGFP-OSH15 gTOB1-mCherry* double reporters. Images of GFP (yellow) and mCherry (magenta) were merged. Bars, 2 cm (B), 200 μ m (D), and 100 μ m (E to L).

spikelet formation (fig S7). Next, we investigated *TOB1/2* expression patterns in developing stems using these reporters. In the wild type, both genes were broadly expressed in leaf primordia but not in the SAM and young stem tissues (Fig. 2E and fig. S8A). Transverse sections revealed that they were broadly expressed beneath the three youngest leaves [plastochron 1 (P1) to P3] (fig. S8, M and P) and continued to be strongly expressed in provascular bundles (PBs) of nodes beneath

P4 to P5, which are the future EVBs (Fig. 2F and fig. S8, B, N, and Q). In the proximal regions corresponding to developing internodes, both genes were repressed (Fig. 2G and fig. S8, C, O, and R). By contrast, *OSH15* and *OSH1* were expressed in all young stem tissues, including PBs (fig. S8, G to L). One exception was their down-regulation in nodal PBs (fig. S8, H and K), in which *TOB1* and *TOB2* were strongly expressed. Observation of *gTOB1-mCherry* and *gGFP-OSH15* double reporters revealed

their complementary accumulation patterns (Fig. 2, K and L). Thus, *TOB1/2* and *OSH15* were expressed in a mutually exclusive manner in wild-type stems.

In *d6* mutants, *TOB1* and *TOB2* were ectopically expressed along PBs; their vascular expressions below the P3 to P5 leaves extended to the bottom of the stem (Fig. 2, H to J, and fig. S8, D to F). Similarly, strong ectopic expression of *TOB1* was observed in stem PBs of *d6 osh1^{+/}* and *ri^{+/} ril* double mutants (fig. S9). Thus, *TOB1/2*

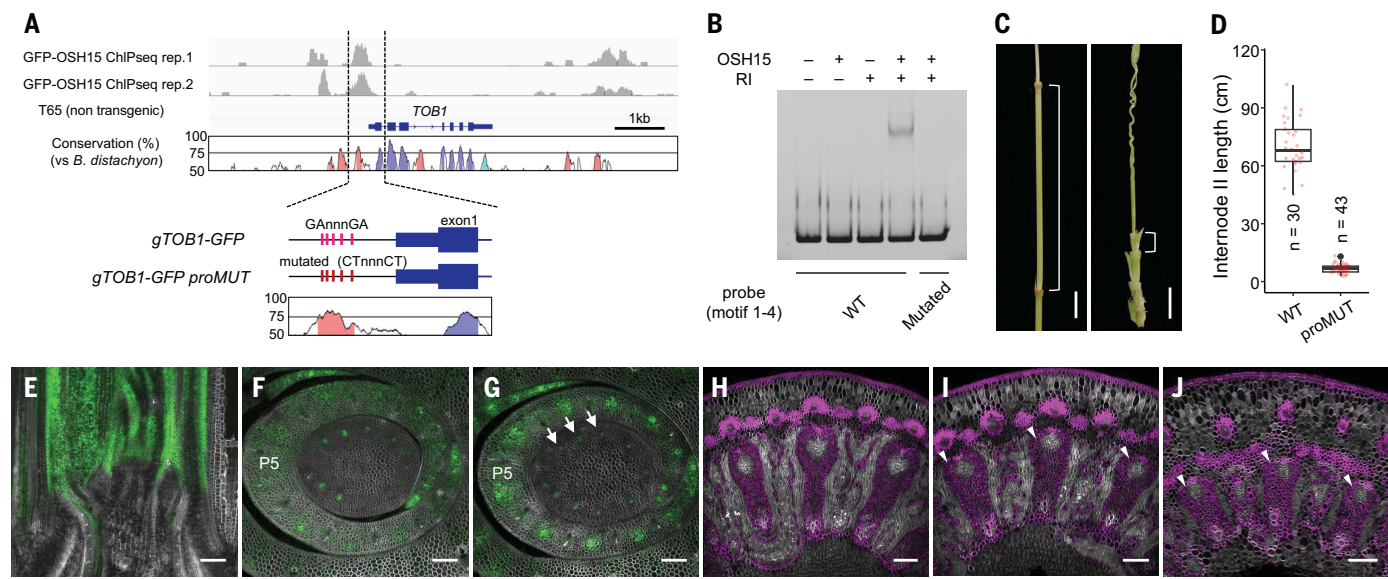


Fig. 3. OSH15 directly represses TOB1 for internode formation. (A) GFP-OSH15 ChIP-seq data at the *TOB1* locus. Nucleotide conservation is shown below the gene model. Putative KNOX1 binding motifs and their mutations in *gTOB1-GFP_promUT* are shown at the bottom. Regions with >75% conservation are colored in pink, blue, and light blue for intergenic, coding, and untranslated regions (UTRs), respectively. (B) Electromobility shift assay using OSH15 and RI proteins and *TOB1* promoter probes comprising putative binding motifs 1 to 4 (fig. S10). In the mutated probe, these motifs were converted into CTnnnCT (fig. S10). (C) Mature stems of *gTOB1-GFP* (left) and *gTOB1-GFP_promUT* (right) plants. Brackets indicate internode II. (D) Internode II length at maturity. P value represents a significant difference (two-sided t test). (E to G) GFP fluorescence (green) in *gTOB1-GFP_promUT* plants. (E) Longitudinal section; (F) transverse section at P4 node; (G) transverse section at P4 internode. Arrows indicate ectopic expressions. (H to J) Transverse sections of *gTOB1-GFP_promUT* mature stems at node I (H), internode II (I), and foot II (J). Arrowheads indicate ectopically formed EVBs. Magenta, basic fuchsin; gray, calcofluor white. Bars, 1 cm (C), 100 μm (E to G), and 200 μm (H to J).

are expressed in nodal PBs and are repressed by KNOX1 and BLH TFs in internodal PBs.

Repression of TOB1 is essential for internode formation

To examine whether OSH15 directly regulates *TOB1*/2 in vivo, we performed chromatin immunoprecipitation (ChIP) assays. We found that OSH15 bound to the *TOB1* promoter and upstream regions of *TOB2* (Fig. 3A and fig. S10A). Previously, we identified the consensus KNOX1 binding motif that comprises two core GAs located three nucleotides apart (GA_nnnGA) (34). Sequence comparisons around the *TOB1* promoter identified five such motifs conserved among grasses (Fig. 3A and fig. S10B). Electrophoretic mobility shift assays showed that the OSH15-RI complex bound to these motifs, whereas neither OSH15 nor RI bound alone, which indicates the requirement of both proteins for binding (Fig. 3B). Mutations in these motifs abolished the binding. Moreover, when these motifs were mutated in the *TOB1* genomic construct (*gTOB1-GFP_promUT*; Fig. 3A), *TOB1* was ectopically expressed in PBs of developing internodes and caused severe dwarfism in the wild type (Fig. 3, C to G, and fig. S10, C to E). Transverse sections revealed that the EVBs occupied the entire stem length at maturity (Fig. 3, H to J). Thus, the repression of *TOB1* by OSH15 is essential for restricting EVB differentiation and allowing internode formation.

Node-specific KNOX1 genes also cause *d6* dwarfism

OSH6 and *OSH71*, two rice genes belonging to the *KNAT2/6* subclade, were also up-regulated in *d6* internodes (fig. S11, A and B). In *Arabidopsis*, *knat6* mutations suppress dwarfisms of *bp* mutants (17). As expected, mutations in *OSH6* and *OSH71* attenuated the *d6* dwarfism, indicating that *OSH15* and *OSH6/71* genetically interact in rice (Fig. 4A and figs. S5 and S11C). A genomic *GFP-OSH71* reporter was expressed in the SAM, in young stems, and at the leaf base in the wild type (Fig. 4K). In later stages, *OSH6* and *OSH71* showed continued expression at nodes but were down-regulated in internodes, which led to node-specific expression patterns (Fig. 4, B to D, and fig. S11D). In *d6* mutants, both genes were ectopically expressed in internodes (Fig. 4, E to G, and fig. S11E). Thus, *OSH6* and *OSH71* are node-specific KNOX1 genes that are repressed by *OSH15*. These results are consistent with those reported in *Arabidopsis*, in which *KNAT2/6* are expressed at organ boundaries and are repressed by *BP* in internodes (17).

OSH6/71 and *TOB1/2* are required for pulvinus formation

osh6 osh71 double mutants showed no obvious abnormality during the vegetative growth. However, they were shorter than the wild type and showed lazy phenotypes after flowering (fig.

S5). They also lacked the pulvinus, a structure that exerts gravitropism at the leaf base in rice (Fig. 4H) (5). Stem bending tests showed that *osh6 osh71* double mutants completely lost stem bending in response to gravity shift (Fig. 4, I and J, and fig. S12A). Pulvini were restored in *gGFP-OSH71 osh6 osh71* plants (fig. S7), which supports the essential function of *OSH71* in pulvinus formation. Unexpectedly, *tob1 tob2* double mutants also failed to form pulvini, although their penetrance was incomplete (32.5%, 13 out of 40). The *tob1 tob2* stems showed varying degrees of bending upon gravity shift. Plants lacking pulvinus were unable to flex the nodes, whereas those with less-severe symptoms could still perform bending (Fig. 4, H to J, and fig. S12A). In the wild-type leaf sheaths, the epidermis and sclerenchymatous bundle caps of veins were highly lignified, and lysigenous aerenchymas were formed between the veins (fig. S12B). In the wild-type pulvini, these aerenchymas were absent, lignification occurred only in the xylem vessels, and collenchymatous bundle caps developed well. In *osh6 osh71* and *tob1 tob2* double mutants that lacked pulvini, all these characteristics of the pulvinus were absent at the leaf base, and the tissue organization was nearly identical to that of the leaf sheath (fig. S12B). Therefore, both *OSH6/71* and *TOB1/2* are important for pulvinus formation. Because their expression domains partially overlap at the leaf base, the pulvinus

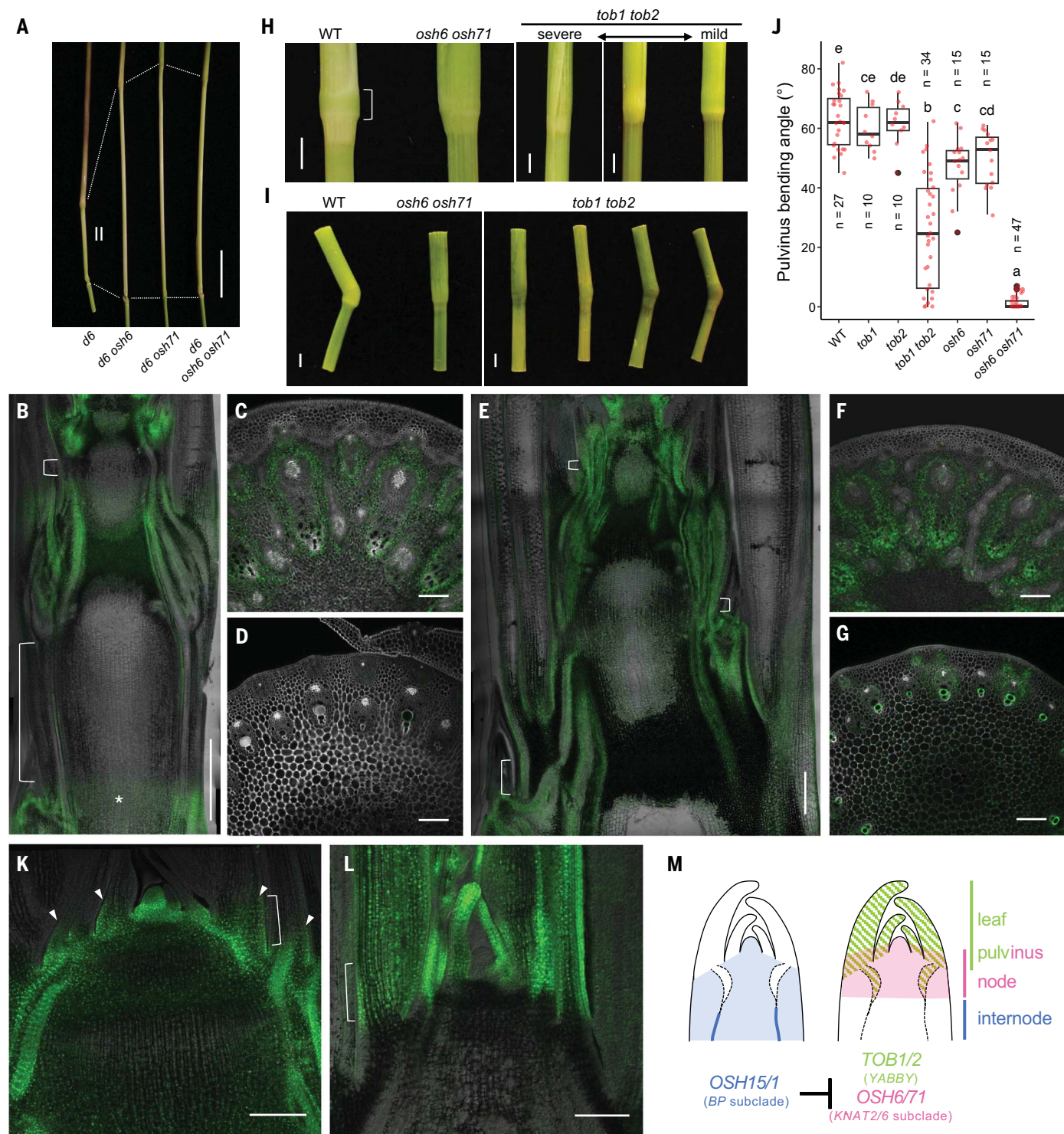


Fig. 4. *OSH6/71* are node-specific *KNOX1* genes essential for pulvinus development. **(A)** Mature internode II in *d6* and *d6 osh6/71* mutants. **(B)** to **(G)** Expression of *gGFP-OSH71* in wild types (**B** to **D**) and *d6* mutants (**E** to **G**). **(B)** and **(E)** show longitudinal sections of developing stems. **(C)**, **(D)**, **(F)**, and **(G)** show transverse sections at nodes (**C**, **F**) and internodes (**D**, **G**). GFP, green; gray, calcofluor white; brackets, internodes; asterisk in **(B)**, *OSH71* expression in the foot. **(H)** Pulvinusless phenotypes of *osh6 osh71* and *tob1 tob2* mutants. **(I)** Pulvinus bending tests. Samples were at 10 days after the onset of gravity shift. **(J)** Measurements of pulvinus bending angles. Different letters indicate significant differences ($P < 0.05$, Tukey–Kramer test). **(K)** and **(L)** *gGFP-OSH71* (**K**) and *gTOB1-GFP* (**L**) expression in the WT shoot apices. Brackets indicate equivalent regions at the leaf base where expression domains of these genes overlap. Arrowheads indicate *GFP-OSH71* accumulation at the base of leaf primordia. **(M)** Model for node–internode patterning. Mutually exclusive expression of *OSH15/1* and *TOB1/2* determines the node–internode pattern, and *OSH6/71* cooperate with *TOB1/2* for pulvinus formation. Bars, 3 cm (**A**), 500 μ m [**(B)** and **(E)**], 100 μ m [**(C)**, **(D)**, **(F)**, and **(G)**], 2 mm [**(H)** and **(I)**], and 200 μ m [**(K)** and **(L)**].

significant differences ($P < 0.05$, Tukey–Kramer test). **(K)** and **(L)** *gGFP-OSH71* (**K**) and *gTOB1-GFP* (**L**) expression in the WT shoot apices. Brackets indicate equivalent regions at the leaf base where expression domains of these genes overlap. Arrowheads indicate *GFP-OSH71* accumulation at the base of leaf primordia. **(M)** Model for node–internode patterning. Mutually exclusive expression of *OSH15/1* and *TOB1/2* determines the node–internode pattern, and *OSH6/71* cooperate with *TOB1/2* for pulvinus formation. Bars, 3 cm (**A**), 500 μ m [**(B)** and **(E)**], 100 μ m [**(C)**, **(D)**, **(F)**, and **(G)**], 2 mm [**(H)** and **(I)**], and 200 μ m [**(K)** and **(L)**].

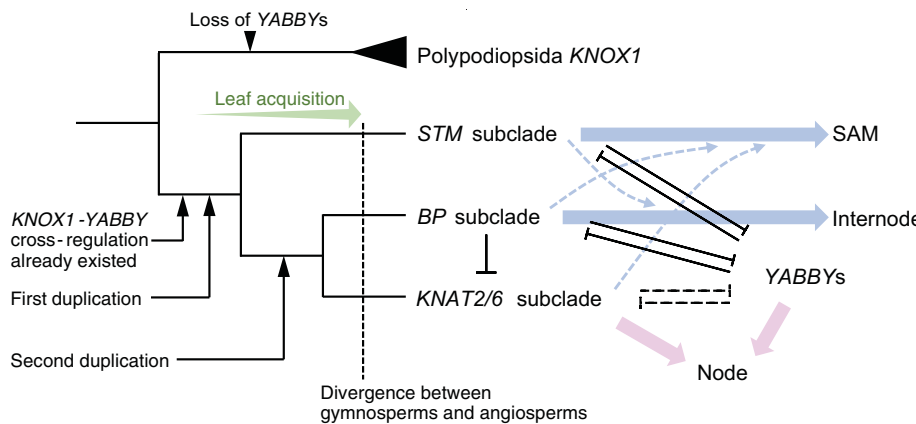


Fig. 5. A model of *KNOX1* subfunctionalization in early seed plants. *YABBY-KNOX1* cross-regulations (possibly mutual repression) likely predated the *KNOX1* duplications, and these events likely occurred before the gymnosperm–angiosperm split. Each *KNOX1* subclade acquired largely specialized but partially overlapping roles along the shoot axis (light blue and pink solid arrows). Dashed arrows in light blue indicate contributions of *KNOX1* genes as reported in (25, 49, 50). The cross-regulation between the *KNAT2/6* subclade and *YABBYs* is likely more derived because they cooperate in node development (dashed black lines). Note that the *YABBY* family is present in Lycopodiales (38) but was lost in Polypodiopsida (35).

is likely formed from a region where both regulators are coexpressed (Fig. 4, K to M).

KNOX1 genes diverged in early seed plants

Our data revealed that cross-regulation among *YABBY* and different *KNOX1* subclades specifies nodes and internodes (Fig. 4M). Because the integration of *YABBY* genes is considered crucial but specific to leaf evolution in seed plants (21, 24, 35), we investigated when these *KNOX1* subclades emerged. We constructed a phylogenetic tree of 453 *KNOX1* proteins from 97 species in land plant lineages. *KNOX1* genes in angiosperms were divided into three groups corresponding to the *SHOOT MERISTEMLESS* (*STM*), *BP*, and *KNAT2/6* subclades (fig. S13). As reported previously, in the commelinids of monocots, *STM* was lost (36, 37) and *BP* was duplicated, possibly for its compensation. Notably, all three *KNOX1* subclades were present in gymnosperms, but not in nonseed plants. Similar topologies have been reported previously (supplementary text); however, the subdivision was not particularly specified (38–40). These data suggest that *KNOX1* duplication likely occurred in early seed plants before the gymnosperm–angiosperm divergence. Notably, *BP* and *KNAT2/6* subclades formed a monophyletic group sister to *STM* (fig. S13). Therefore, the first duplication of the ancient *KNOX1* gene likely generated *STM* and another gene, and the second duplication of the latter gave rise to *BP* and *KNAT2/6* subclades (Fig. 5).

Discussion

We propose that nodes and internodes are distinct domains specified by the *YABBY-KNOX1* cross-regulations that diverged in early seed plants (Figs. 4M and 5). Because

YABBY genes repress all three *KNOX1* subclades in *Arabidopsis* leaves (20), and the complementary expression patterns of these genes are widely observed in seed plants (21, 41–43), the *YABBY-KNOX1* cross-regulation was likely present before *KNOX1* duplication and the divergence between gymnosperms and angiosperms. Given that early seed plants had leafless and three-dimensionally branching axes (18, 19), the ancient *KNOX1* gene likely contributed to the SAM and internodes before leaf evolution. As determinacy in the lateral branching system and lamina growth became more pronounced through the integration of *YABBY* genes into the leaf program (21, 24), this cross-regulation may have increased its importance. *STM* and *BP* genes likely inherited functions in the SAM and internodes, which enabled robust but separable regulation along the shoot axis. *KNAT2/6* genes are more derived because they act antagonistically to *BP* and are partially coexpressed with *YABBY* genes, adding complexity to *YABBY-KNOX1* cross-regulation and nodal structures. Although our data suggested that these *KNOX1* subclades emerged in early seed plants, whether they play similar roles in gymnosperms remains to be tested.

Mutually exclusive expression of *TOB1/2* and *OSH15/1* delimits the nodes and internodes (Fig. 4M). Vascular differentiation likely plays key roles in this context. The expression of *TOB1/2* along PBs induces the formation of nodal EVBs, and their repression is pivotal for internodes. Notably, the ectopic expression of *TOB1/2* in *knox1/blh* mutants and *gTOB1-GFP_promUT* plants was limited to the PBs of internodes, but their developmental consequences extended beyond vasculatures. Therefore, *TOB1/2* expressed in the PBs likely regulate

the differentiation of the surrounding tissues non-cell autonomously, possibly through downstream targets. In *Arabidopsis*, the non-cell autonomous action of *FIL* is known to affect phyllotaxis by way of the organ boundary gene *LATERAL SUPPRESSOR* (44). Additionally, vascular expression of *YABBY* genes has been reported in several species and is also known to regulate vascular stem cell fate (38, 43, 45, 46). One caveat is that we have observed no clear defects in *tob1 tob2* EVBs. Further studies, in combination with other *YABBY* mutations, are required to establish their functions in EVB and node formation.

Genetic interactions among *BP*, *KNAT2/6*, and *FIL* in *Arabidopsis* (14, 17) and the dwarfism caused by dominant *FIL* mutations in cucurbits (47) suggest that similar mechanisms for stem development operate in a wide range of species. Indeed, we found that putative *KNOX1*-binding sites are conserved in the 5' regions of *FIL* orthologs in dicots (fig S14). Additionally, *BLADE ON PETIOLE* genes are likely involved in this process because they also genetically interact with *BP* (15, 16). Other regulators that function in related contexts, such as organ boundaries, leaf polarities, and vascular differentiation, may also participate in node–internode patterning.

The pulvinus is recognized as a part of the leaf because of its morphological and clonal continuity with the leaf sheath (supplementary text) (5, 48). However, we showed that pulvinus development requires both *TOB1/2* and *OSH6/71*, suggesting that it can be assigned to both nodes and leaves (Fig. 4M). The foot was another domain with unclear identity. Because it is marked by *OSH6/71* expression (Fig. 4B), the foot likely shares developmental programs with the nodes. Indeed, both domains are achlorophyllous and nonelongating, and develop vascular connections between the stem and lateral organs (fig. S1 and supplementary text) (5). As far as we observed, *osh6 osh71* stems are normal except for the pulvinus, indicating the presence of additional factors important for node and foot development.

Given that cis-regulatory mutations in *TOB1* can affect stem length, it will be interesting to seek optimal alleles that achieve a desired height. Further efforts to understand the genetic basis of stem development and fine-tune its regulators would allow us to manipulate crop height for agricultural improvement.

REFERENCES AND NOTES

1. N. Yamaji, J. F. Ma, *Curr. Opin. Plant Biol.* **39**, 18–24 (2017).
2. Á. Ferrero-Serrano, C. Cantos, S. M. Assmann, *Cold Spring Harb. Perspect. Biol.* **11**, a034645 (2019).
3. A. Serrano-Mislata, R. Sablowski, *Curr. Opin. Plant Biol.* **45** (Pt A), 11–17 (2018).
4. W. Tanaka, T. Yamauchi, K. Tsuda, *Breed. Sci.* **73**, 3–45 (2023).
5. K. Tsuda, A. Maeno, K. I. Nonomura, *Plant Cell* **35**, 4366–4382 (2023).
6. A. Serrano-Mislata et al., *Nat. Plants* **3**, 749–754 (2017).
7. A. Hay, M. Tsiantis, *Development* **137**, 3153–3165 (2010).

8. S. J. Douglas, G. Chuck, R. E. Dengler, L. Pelecanas, C. D. Riggs, *Plant Cell* **14**, 547–558 (2002).
9. J. A. Long, E. I. Moan, J. I. Medford, M. K. Barton, *Nature* **379**, 66–69 (1996).
10. Y. Sato *et al.*, *EMBO J.* **18**, 992–1002 (1999).
11. H. M. Smith, S. Hake, *Plant Cell* **15**, 1717–1727 (2003).
12. K. Tsuda *et al.*, *Plant Cell* **29**, 1105–1118 (2017).
13. S. Bencivenga, A. Serrano-Mislata, M. Bush, S. Fox, R. Sablowski, *Dev. Cell* **39**, 198–208 (2016).
14. S. J. Douglas, B. Li, D. J. Kliebenstein, E. Nambara, C. D. Riggs, *PLOS ONE* **12**, e0177045 (2017).
15. M. Khan *et al.*, *Plant Physiol.* **169**, 2166–2186 (2015).
16. M. Khan *et al.*, *Plant Physiol.* **158**, 946–960 (2012).
17. L. Ragni, E. Belles-Boix, M. Günl, V. Pautot, *Plant Cell* **20**, 888–900 (2008).
18. H. Sanders, G. W. Rothwell, S. E. Wyatt, *Int. J. Plant Sci.* **170**, 860–868 (2009).
19. A. M. Tomescu, *Trends Plant Sci.* **14**, 5–12 (2009).
20. M. K. Kumaran, J. L. Bowman, V. Sundaresan, *Plant Cell* **14**, 2761–2770 (2002).
21. R. Sarojam *et al.*, *Plant Cell* **22**, 2113–2130 (2010).
22. S. Sawa *et al.*, *Genes Dev.* **13**, 1079–1088 (1999).
23. K. R. Siegfried *et al.*, *Development* **126**, 4117–4128 (1999).
24. S. K. Floyd, J. L. Bowman, *Int. J. Plant Sci.* **168**, 1–35 (2007).
25. K. Tsuda, Y. Ito, Y. Sato, N. Kurata, *Plant Cell* **23**, 4368–4381 (2011).
26. T. Ikeda *et al.*, *Plant J.* **98**, 465–478 (2019).
27. K. I. Hibara *et al.*, *PLOS Genet.* **17**, e1009292 (2021).
28. Z. Hong *et al.*, *Plant J.* **32**, 495–508 (2002).
29. J. I. Itoh, A. Hasegawa, H. Kitano, Y. Nagato, *Plant Cell* **10**, 1511–1522 (1998).
30. J. Wang *et al.*, *Plant J.* **91**, 85–96 (2017).
31. G. Mele, N. Ori, Y. Sato, S. Hake, *Genes Dev.* **17**, 2088–2093 (2003).
32. W. Tanaka, T. Toriba, H. Y. Hirano, *New Phytol.* **215**, 825–839 (2017).
33. W. Tanaka *et al.*, *Plant Cell* **24**, 80–95 (2012).
34. K. Tsuda, N. Kurata, H. Ohyanagi, S. Hake, *Plant Cell* **26**, 3488–3500 (2014).
35. M. A. Romanova, A. I. Maksimova, K. Pawlowski, O. V. Voitsekhovskaja, *Int. J. Mol. Sci.* **22**, 4139 (2021).
36. Y. Hirayama *et al.*, *Dev. Genes Evol.* **217**, 363–372 (2007).
37. S. Jouannic, M. Collin, B. Vidal, J. L. Verdeil, J. W. Trengear, *New Phytol.* **174**, 551–568 (2007).
38. A. I. Evkaikina *et al.*, *Genome Biol. Evol.* **9**, 2444–2460 (2017).
39. C. Furumizu, J. P. Alvarez, K. Sakakibara, J. L. Bowman, *PLOS Genet.* **11**, e1004980 (2015).
40. K. Sakakibara, T. Nishiyama, H. Deguchi, M. Hasebe, *Evol. Dev.* **10**, 555–566 (2008).
41. G. Bharathan *et al.*, *Science* **296**, 1858–1860 (2002).
42. C. Finet *et al.*, *Evol. Dev.* **18**, 116–126 (2016).
43. T. Yamada *et al.*, *Plant J.* **67**, 26–36 (2011).
44. A. Goldshmidt, J. P. Alvarez, J. L. Bowman, Y. Eshed, *Plant Cell* **20**, 1217–1230 (2008).
45. A. M. Nurani *et al.*, *Plant Cell Physiol.* **61**, 255–264 (2020).
46. T. Toriba *et al.*, *Mol. Genet. Genomics* **277**, 457–468 (2007).
47. S. Wang *et al.*, *Nat. Plants* **8**, 1394–1407 (2022).
48. W. V. Brown, G. A. Pratt, H. M. Mobley, *Southwest. Nat.* **4**, 126–130 (1959).
49. E. Belles-Boix *et al.*, *Plant Cell* **18**, 1900–1907 (2006).
50. M. E. Byrne, J. Simorowski, R. A. Martienssen, *Development* **129**, 1957–1965 (2002).

ACKNOWLEDGMENTS

We thank M. Kashihara for field management, S. Hake for thoughtful comments on the manuscript, M. Endo for providing the genome editing vectors, and H. Hirano for providing *tob1*, *ri*, and *ril* seeds. Computations were partially performed on the NIG supercomputer at ROIS National Institute of Genetics. **Funding:** Japan Society for the Promotion of Science (JSPS) KAKENHI 18H04845 (K.T.); JSPS KAKENHI 20H04891 (K.T.); JSPS KAKENHI 22H02319 (K.T.); JSPS KAKENHI 23H04754 (K.T.); JSPS KAKENHI 21H04729 (K.-I.N.). **Author contributions:** Conceptualization: K.T.; Methodology: K.T. and A.M.; Investigation: K.T., A.M., A.O., K.K., W.T., and K.-I.H.; Visualization: K.T.; Funding acquisition: K.T. and K.-I.N.; Project administration: K.T.; Supervision: K.T. and K.-I.N.; Writing – original draft: K.T.; Writing – review and editing: K.T., A.M., W.T., K.-I.H., and K.-I.N. **Competing interests:** The authors declare that they have no competing interests. **Data and materials availability:** Transcriptome and ChIP-sequencing data are available in the DDBJ Sequence Read Archive under the accession numbers PRJDB13390 and PRJDB16754, respectively. All other data are available in the main text or the supplementary materials. All materials are available upon request from the corresponding author. **License information:** Copyright © 2024 the authors, some rights reserved; exclusive licensee American Association for the Advancement of Science. No claim to original US government works. <https://www.scienmag.org/about/science-licenses-journal-article-reuse>

SUPPLEMENTARY MATERIALS

science.org/doi/10.1126/science.adn6748

Materials and Methods

Supplementary Text

Figs. S1 to S14

Tables S1 to S3

References (51–77)

MDAR Reproducibility Checklist

Data S1 to S5

Submitted 22 December 2023; accepted 3 May 2024
10.1126/science.adn6748